Supporting Information for:

Changes in inorganic fine particulate matter sensitivities to precursors due to large-scale US emissions reductions

Jareth Holt[1*], Noelle E. Selin[1,2], Susan Solomon[1]

1 Department of Earth, Atmospheric and Planetary Sciences, Massachusetts Institute of Technology, Cambridge, MA, USA

2 Engineering Systems Division, Massachusetts Institute of Technology, Cambridge, MA 02139, USA

* Corresponding author contact information:

77 Massachusetts Ave

Bldg 54-1711

Cambridge, MA 02139

Phone: +1 617 253 6281

Fax: +1 617 258 7733

Email: jareth@mit.edu

Contents: 18 pages, 7 figures, 2 tables.

PM2.5 COMPONENT CONCENTRATIONS. **Figure S1** and **Figure S2** show the simulated surface concentrations of the individual inorganic $PM_{2.5}$ components (NO_3^-, $SO_4^=$, and NH_4^+) in January and July, respectively.

January $PM_{2.5}$ is composed primarily of ammonium nitrate in most of the country. Only the southeastern US has substantial $SO_4^=$ concentrations. The differences between the high and low emissions cases largely reflect this regional description, with reductions in both NO_3^- and NH_4^+ in the northern Midwest and $SO_4^=$ reductions in the southeast. However, there is a region of the eastern US (around Virginia, Kentucky, and Ohio) where NO_3^- concentrations are actually higher in the low emissions case. This behavior has been described before[1] and is due to lower $SO_4^=$ concentrations allowing gaseous nitric acid to condense and form NO_3^-.

July $PM_{2.5}$ has more $SO_4^=$ and less NO_3^- than January $PM_{2.5}$. $SO_4^=$ concentrations broadly cover the eastern US, and the differences in $SO_4^=$ between the high and low emissions cases are centered around the Ohio river valley (the location of US SO_2 sources). NH_4^+ concentrations and reductions mirror those of $SO_4^=$. Modeled July NO_3^- concentrations can reach 5 $\mu g\ m^{-3}$ in the high emissions case in the region south of the Great Lakes (Michigan, Indiana, Ohio) and some urban areas.

GEOS-CHEM MODEL EVALUATION. We evaluated model performance by comparing concentrations of inorganic $PM_{2.5}$ components in our 2005 simulation (high emissions case) to measurements in January and July of 2005 from two monitoring networks: the Interagency Monitoring of Protected Visual Environments (IMPROVE) network[2] and the US EPA's Air Quality System (AQS)[3]. IMPROVE focuses on rural environments and takes 24-hour average measurements once every 3 days; AQS includes

urban monitoring sites and provides 24-hour average $PM_{2.5}$ speciation every day. The aggregate statistics shown in Table S1 and Table S2 compare the 24-hour measurement for a site and day with the 24-hour average GEOS-Chem concentration on that day from the grid cell containing that site. In other words, the statistical comparison has been paired in both time and space. For details on the statistics calculated, see Simon, Baker, and Phillips[4]. The scatterplot comparisons, **Figure S3** and **Figure S4**, show monthly means from GEOS-Chem and the measurement networks, with gray lines denoting the inter-quartile range of the 24-hour averages over that month. They show only spatial pairing, but with the temporal variability indicated by the lines.

Our simulation agrees well with $SO_4^=$ measurements. In January, the modeled $SO_4^=$ concentrations are unbiased (NMB<5%) but with modest correlation (r^2=30.8% compared to IMPROVE). In the northern Midwest, however, modeled January $SO_4^=$ is low (NMB=-45%). In July, the spatial correlation is much higher (r^2=67.3%) but modeled $SO_4^=$ is low (NMB of –10% to –20%). Modeled NH_4^+ is high compared to measurements (NMB of 0 to 89%) with modest correlation (r^2 of 10.7% to 43.1%). Compared to NO_3^- measurements, the model is biased very high: NMB between 86% and 133% in January and 70% in July. The correlation is modest in January (r^2=39% compared to IMPROVE) but extremely low in July (r^2=3% compared to AQS).

The high bias of GEOS-Chem aerosol NO_3^- has been explored previously[5–7] but our comparison highlights a few interesting details. The modeled winter concentrations has a higher correlation with the rural IMPROVE measurements than with the more urban AQS measurements but the bias is larger as well. The spatial and temporal agreement with rural measurements suggests that the model captures the large-scale

spatial structure of nitrate formation but overestimates HNO_3 production or underestimates its atmospheric removal.

SO2 OXIDATION PATHS. Figure 4 in the main paper showed the ratio of the aqueous and gaseous SO_2 oxidation rates. We argued that the larger aqueous fraction of SO_2 oxidation and larger $PM_{2.5}$ sensitivity to SO_2 emissions in the low emissions case was due to the lower NO_x emissions. This conclusion is reinforced by the OH, HO_2, and H_2O_2 concentrations (**Figure S5**), which show lower OH and higher HO_2, H_2O_2 concentrations in the low emissions case than the high emissions case. H_2O_2 is produced by the reaction of HO_2 (or other peroxy radicals) with itself, whereas NO_x catalyzes the transformation of HO_2 into OH. With low NO_x concentrations, more HO_x is in the form of HO_2, allowing the self-reaction to form H_2O_2, which then oxidizes SO_2.

A change in the production pathway of $SO_4^=$ could also lead to a change in its deposition rate which would also affect $PM_{2.5}$ concentrations. In particular, more aqueous-phase oxidation could promote more wet deposition of sulfate. **Figure S6** shows the wet deposition rates of both SO_2 and $SO_4^=$ in our simulations. The rates were calculated as the total wet deposition over the month divided by the column burden of the species, controlling for the difference in SO_2 emissions and hence total sulfur between the two cases. $SO_4^=$ wet deposition rates are broadly similar between the two cases but typically smaller in the low emissions case. January SO_2 wet deposition rates are generally larger in the low emissions case than the high emissions case whereas January deposition rates are smaller. The change in wet deposition rates suggests that $SO_4^=$ may have a longer lifetime in the atmosphere in the low emissions case in addition to being produced more rapidly from SO_2. At the very least, the larger aqueous oxidation rate in

the low emissions case is not compensated by more wet deposition and hence the sensitivity of $PM_{2.5}$ to SO_2 emissions is larger.

ERRORS IN USING CONSTANT SENSITIVITIES. Since $PM_{2.5}$ sensitivities in the high and low emissions cases differ, this implies (by definition) that a constant-sensitivity model will display some error. Figure S7 shows the $PM_{2.5}$ concentrations that would be predicted for the low emissions case, given the high emissions case $PM_{2.5}$ sensitivities and concentrations. That is, it shows how a linear extrapolation from a few simulations, each slightly varying NEI05 emissions, would predict the results of the low emissions simulation. This kind of extrapolation is sometimes necessary as emissions inventories take years to compile and high-resolution air quality models are too computationally expensive to run over the entire potential range of emissions.

The linear model shows deviations of ~10% from the actual simulation in the central and southeast US in January. In July, the constant-sensitivity model deviates by 15% in most of the eastern US and by up to 25% in the mid-Atlantic coast. Elsewhere, the constant-sensitivity model is reasonably accurate. The constant-sensitivity model consistently overestimates the concentrations, translating into an underestimate of the benefits of emissions reductions.

We have emphasized the errors in the constant-sensitivity model but the 15-25% overestimates of $PM_{2.5}$ come from applying a linear model to ~50% changes in two of the three emissions. The general agreement between the constant-sensitivity model and the full simulation is mainly due to the assumed lack of change in NH_3 emissions. The large differences in NH_3 sensitivities between the high and low emissions cases have no impact on the model predictions if NH_3 emissions stay constant. If NH_3 emissions were lowered

93 from the low emissions case, however, then $PM_{2.5}$ reductions would be much smaller than
94 predicted from the constant-sensitivity model.

REFERENCES

(1) West, J.; Ansari, A.; Pandis, S. Marginal PM2.5 : Nonlinear Aerosol Mass Response to Sulfate Reductions in the Eastern United States. *J. Air Waste Manage. Assoc.* **1999**, *49*, 1415–1424.

(2) Malm, W. C.; Sisler, J. F.; Huffman, D.; Eldred, R. A.; Cahill, T. A. Spatial and seasonal trends in particle concentration and optical extinction in the United States. *J. Geophys. Res.* **1994**, *99*, 1347.

(3) US Environmental Protection Agency.Daily summary data for particulates. http://aqsdr1.epa.gov/aqsweb/aqstmp/airdata/download_files.html#Daily (accessed Nov 24, 2014).

(4) Simon, H.; Baker, K. R.; Phillips, S. Compilation and interpretation of photochemical model performance statistics published between 2006 and 2012. *Atmos. Environ.* **2012**, *61*, 124–139.

(5) Walker, J. M.; Philip, S.; Martin, R. V.; Seinfeld, J. H. Simulation of nitrate, sulfate, and ammonium aerosols over the United States. *Atmos. Chem. Phys.* **2012**, *12*, 11213–11227.

(6) Heald, C. L.; Collett, J. L. J.; Lee, T.; Benedict, K. B.; Schwandner, F. M.; Li, Y.; Clarisse, L.; Hurtmans, D. R.; Van Damme, M.; Clerbaux, C.; et al. Atmospheric ammonia and particulate inorganic nitrogen over the United States. *Atmos. Chem. Phys.* **2012**, *12*, 10295–10312.

(7) Zhang, L.; Jacob, D. J.; Knipping, E. M.; Kumar, N.; Munger, J. W.; Carouge, C. C.; van Donkelaar, A.; Wang, Y. X.; Chen, D. Nitrogen deposition to the United States: distribution, sources, and processes. *Atmos. Chem. Phys.* **2012**, *12*, 4539–4554.

(8) Fountoukis, C.; Nenes, A. ISORROPIA II: a computationally efficient thermodynamic equilibrium model for K+–Ca2+–Mg2+–NH4+–Na+–SO42−–NO3−–Cl−–H2O aerosols. *Atmos. Chem. Phys.* **2007**, *7*, 4639–4659.

(9) Vayenas, D. V.; Takahama, S.; Davidson, C. I.; Pandis, S. N. Simulation of the thermodynamics and removal processes in the sulfate-ammonia-nitric acid system during winter: Implications for PM2.5 control strategies. *J. Geophys. Res. Atmos.* **2005**, *110*, No. D07S14.

TABLES

Table S1. Statistical comparison of modeled and measured $PM_{2.5}$ species concentrations for January 2005. N is the number of sites and days with valid data for the comparison; MB, ME, and RMSE are the mean bias, mean error, and root mean square error; FB, FE, NMB, and NME are the fractional bias, fractional error, normalized mean bias, and normalized mean error; and r^2 is the squared correlation coefficient.

Table S2. Same as Table S1 but for July 2005.

Jan		N	MB $\mu g\ m^{-3}$	ME $\mu g\ m^{-3}$	RMSE $\mu g\ m^{-3}$	FB %	FE %	NMB %	NME %	r^2 %
NO_3^-	IMP	1722	1.47	1.88	3.36	35.1	110.8	133.8	171.3	39.0
	AQS	575	0.84	1.54	2.72	7.4	118.3	86.0	158.3	16.1
$SO_4^=$	IMP	1724	-0.00	0.74	1.33	24.1	67.1	-0.3	59.2	30.8
	AQS	605	0.05	0.89	1.72	19.4	73.0	4.6	75.4	17.0
NH_4^+	IMP	141	0.45	0.55	0.70	43.9	54.5	51.0	61.3	43.1
	AQS	13	0.75	0.91	1.55	48.7	61.8	89.1	107.9	34.8

Table S1. Statistical comparison of modeled and measured $PM_{2.5}$ species concentrations for January 2005. N is the number of sites and days with valid data for the comparison; MB, ME, and RMSE are the mean bias, mean error, and root mean square error; FB, FE, NMB, and NME are the fractional bias, fractional error, normalized mean bias, and normalized mean error; and r^2 is the squared correlation coefficient.

Jul		N	MB μg m^{-3}	ME μg m^{-3}	RMSE μg m^{-3}	FB %	FE %	NMB %	NME %	r^2 %
NO_3^-	IMP	1514	0.19	0.46	1.28	-12.3	99.3	70.3	172.9	0.8
	AQS	514	0.18	0.43	1.09	-21.4	102.6	70.1	167.8	3.2
$SO_4^=$	IMP	1514	-0.48	1.19	2.09	1.6	47.9	-17.6	43.1	67.3
	AQS	580	-0.29	1.51	2.68	4.6	57.0	-10.9	57.2	39.5
NH_4^+	IMP	27	-0.00	0.70	0.87	1.0	36.2	-0.1	34.9	23.2
	AQS	23	0.60	1.06	1.65	35.2	58.5	48.0	85.0	10.7

Table S2. Same as **Table S1** but for July 2005.

FIGURES

Figure S1. January concentrations of the inorganic $PM_{2.5}$ components NO_3^-, $SO_4^=$, and NH_4^+, as well as the total $PM_{2.5}$ concentrations. The first and second columns shows results from the high emissions (NEI05) and low emissions (2012 analogue) cases, respectively; the third column shows their difference.

Figure S2. Same as Figure 1, but for July.

Figure S3. GEOS-Chem grid cell concentrations of inorganic $PM_{2.5}$ components compared to IMPROVE measurements. The error bars show the inter-quartile range (IQR) of the month of measurements; dots show the monthly mean.

Figure S4. Same as Figure 3, but for the AQS measurements.

Figure S5. Concentrations of the oxidants OH, HO_2, and H_2O_2 in our simulations. The format is the same as in Figure 1 and Figure 2, with a fourth column comparing the grid point values in the high and low emissions cases to each other.

Figure S6. Average wet deposition rates for SO_2 and $SO_4^=$. The rates here are calculated as the monthly-total wet deposition in each grid cell (mol), divided by the species burden (column sum concentration, mol m^{-2}), the grid cell surface area (m^2) and the averaging period (1 month=2.7×10^6 s) to get a rate in units of s^{-1}.

Figure S7. Comparison of the $PM_{2.5}$ concentrations in the low emissions case to a linear extrapolation based on the concentrations and sensitivities in the high emissions case.

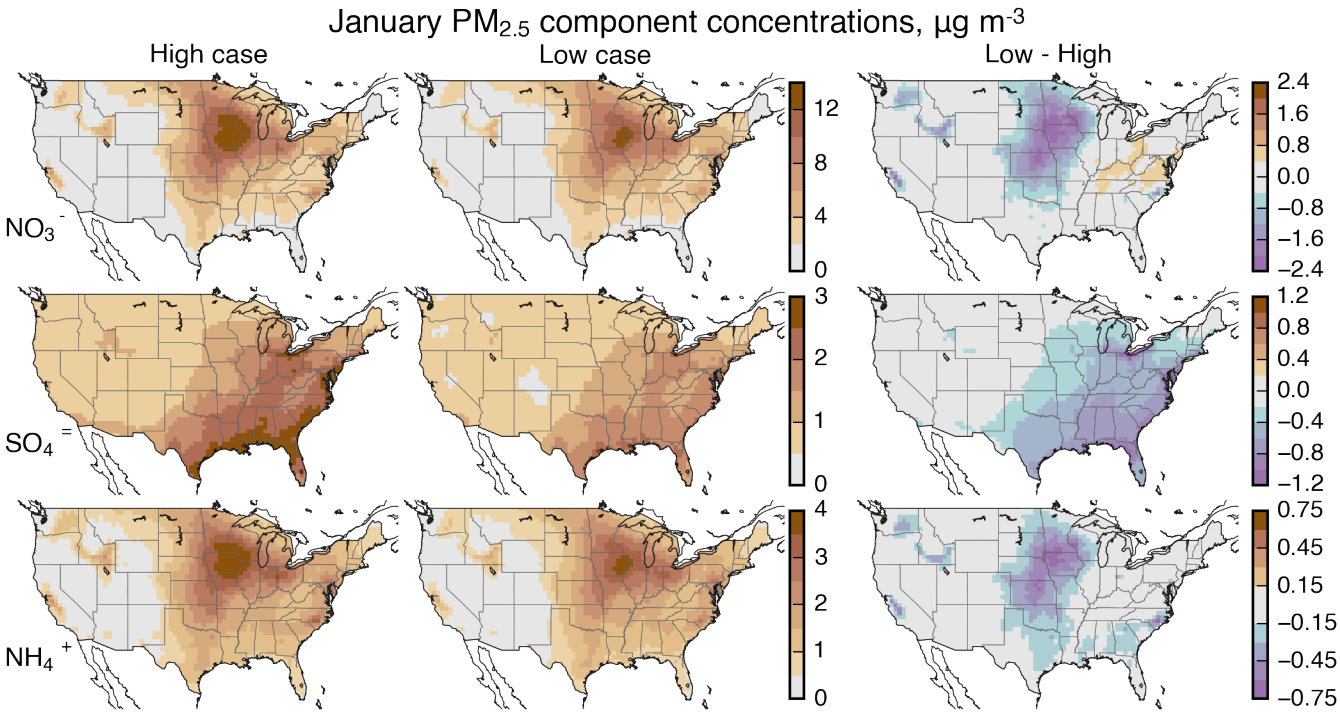

Figure S1. January concentrations of the inorganic $PM_{2.5}$ components NO_3^-, $SO_4^=$, and NH_4^+, as well as the total $PM_{2.5}$ concentrations. The first and second columns shows results from the high emissions (NEI05) and low emissions (2012 analogue) cases, respectively; the third column shows their difference.

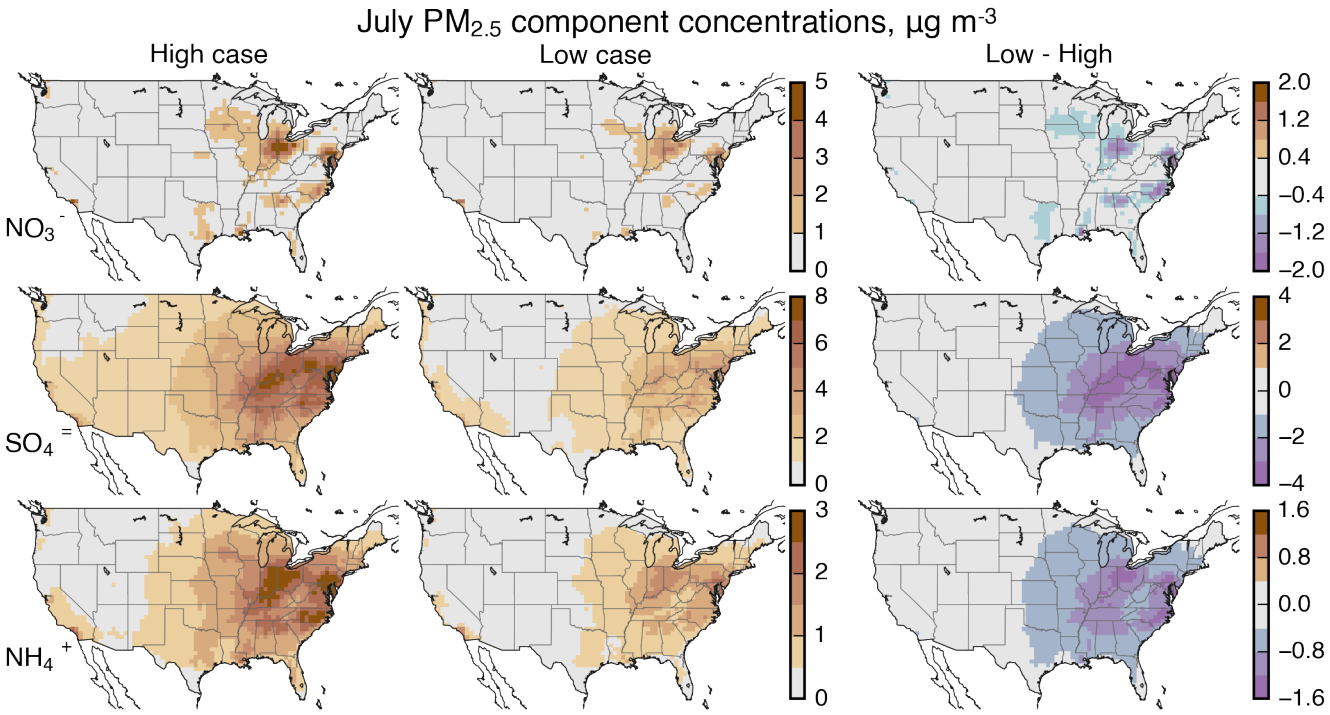

Figure S2. Same as **Figure S1**, but for July.

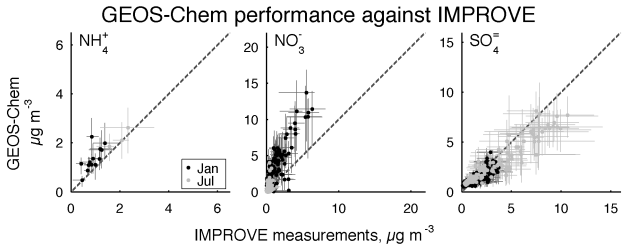

Figure S3. GEOS-Chem grid cell concentrations of inorganic $PM_{2.5}$ components compared to IMPROVE measurements. The error bars show the inter-quartile range (IQR) of the month of measurements; dots show the monthly mean.

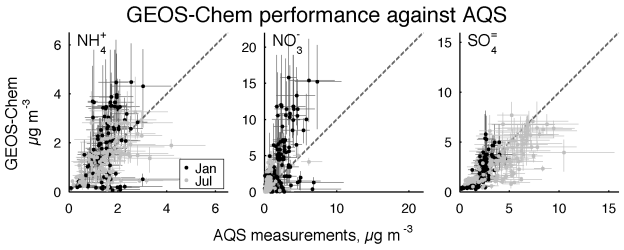

Figure S4. Same as **Figure S3**, but for the AQS measurements.

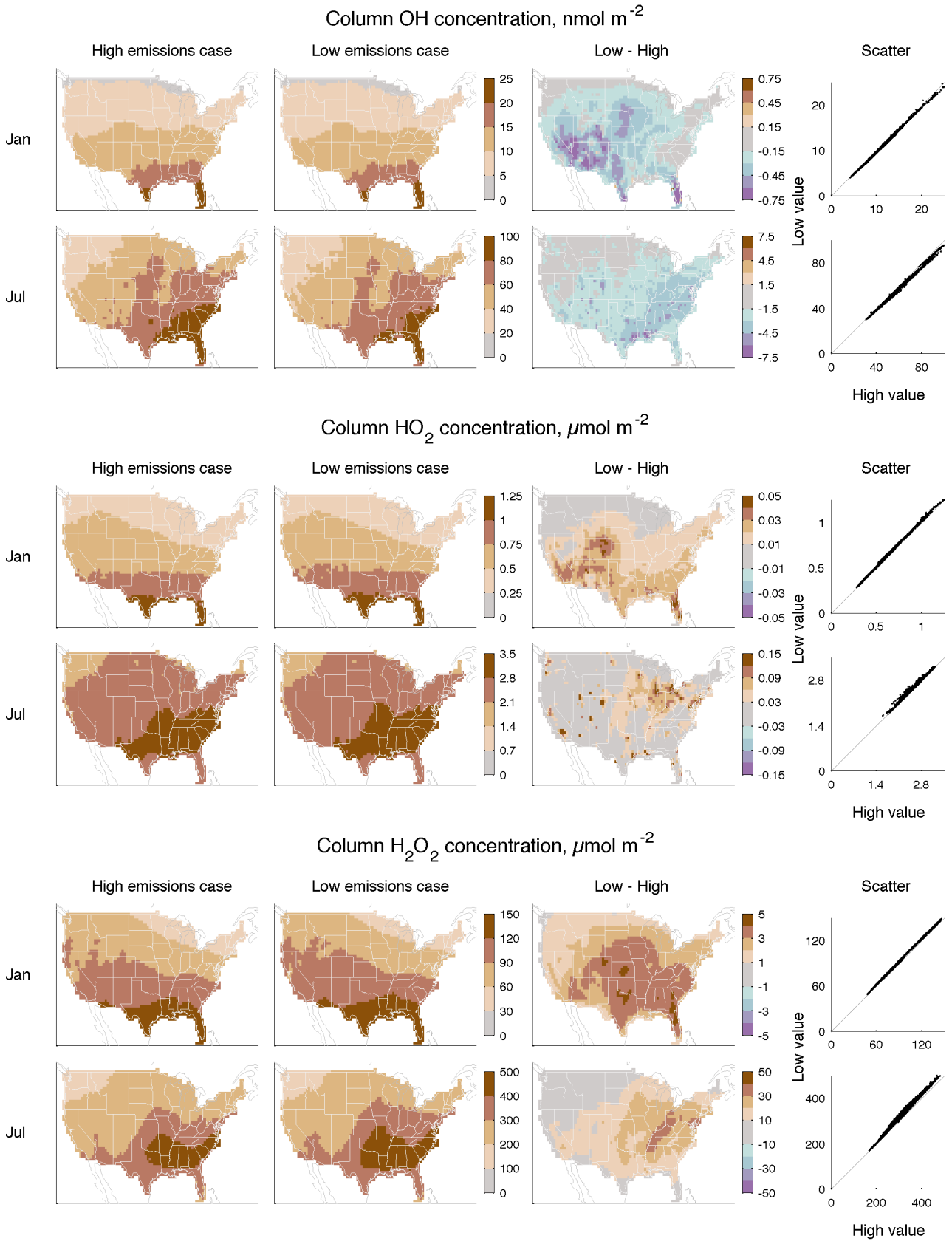
Column OH concentration, nmol m-2
High emissions case
Low emissions case
Low - High
Scatter
Jan
Jul
25
20
15
10
5
0
0.75
0.45
0.15
-0.15
-0.45
-0.75
100
80
60
40
20
0
7.5
4.5
1.5
-1.5
-4.5
-7.5
Low value
High value
Column HO2 concentration, μmol m-2
1.25
1
0.75
0.5
0.25
0.05
0.03
0.01
-0.01
-0.03
-0.05
3.5
2.8
2.1
1.4
0.7
0.15
0.09
0.03
-0.03
-0.09
-0.15
Column H2O2 concentration, μmol m-2
150
120
90
60
30
5
3
1
-1
-3
-5
500
400
300
200
100
50
30
10
-10
-30
-50

Figure S5. Concentrations of the oxidants OH, HO_2, and H_2O_2 in our simulations. The format is the same as in **Figure S1** and **Figure S2**, with a fourth column comparing the grid point values in the high and low emissions cases to each other.

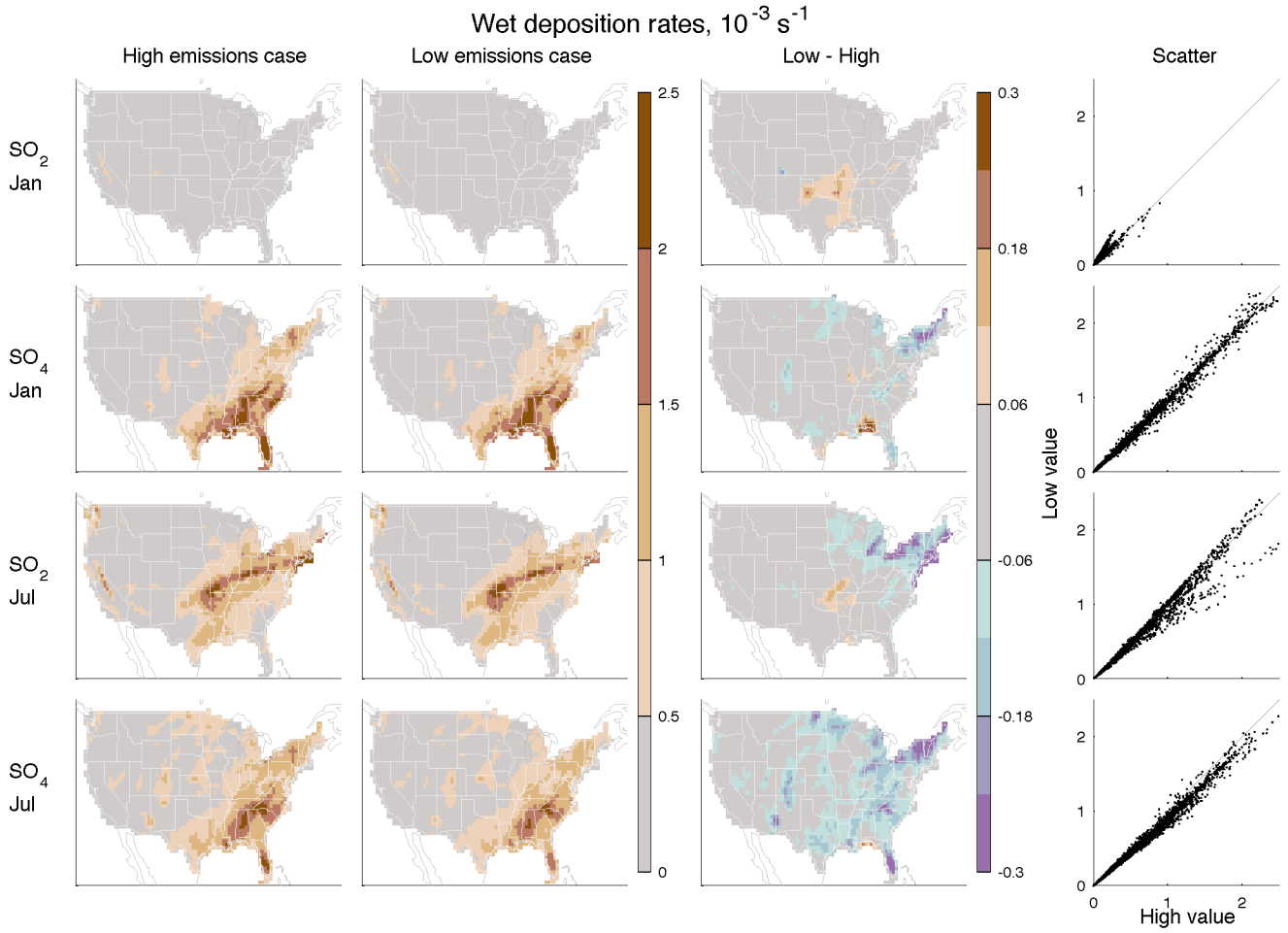

Figure S6. Average wet deposition rates for SO_2 and $SO_4^=$. The rates here are calculated as the monthly-total wet deposition in each grid cell (mol), divided by the species burden (column sum concentration, mol m^{-2}), the grid cell surface area (m^2) and the averaging period (1 month=2.7×10^6 s) to get a rate in units of s^{-1}.

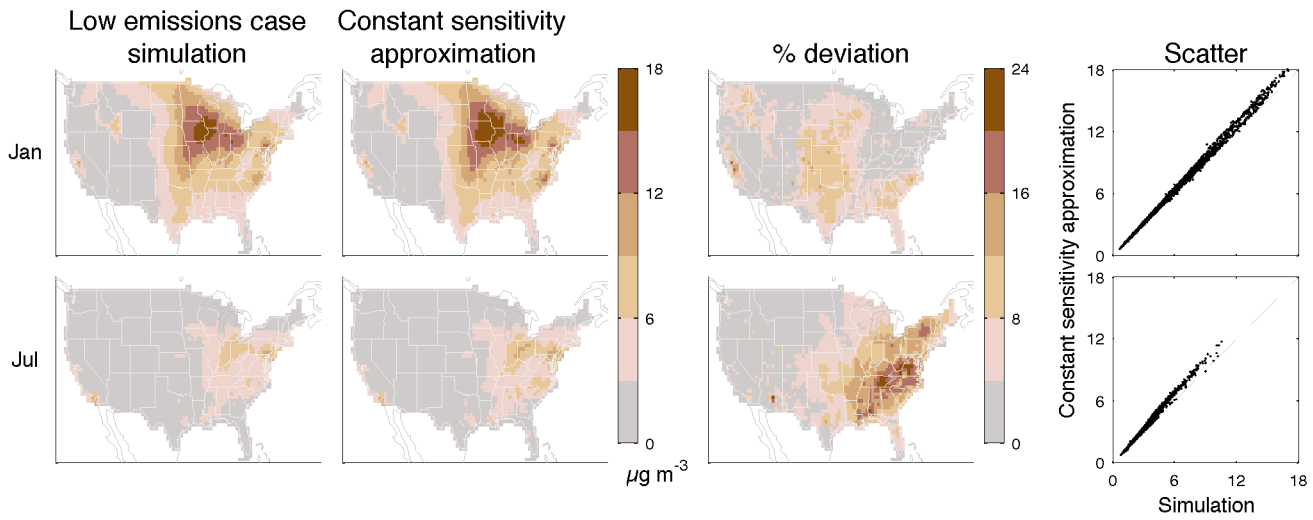

Figure S7. Comparison of the $PM_{2.5}$ concentrations in the low emissions case to a linear extrapolation based on the concentrations and sensitivities in the high emissions case.